IOP Publishing Journal of Physics D: Applied Physics
J. Phys. D: Appl. Phys. **46** (2013) 495110 (7pp) doi:10.1088/0022-3727/46/49/495110

Organic field-effect transistors: predictive control on performance parameters

K Datta[1,5], P Ghosh[1,5], Ashok Mulchandani[2], Sung-Hwan Han[3], P Koinkar[4] and Mahendra D Shirsat[1,6]

[1] Intelligent Materials Research Laboratory, Department Of Physics, Dr. Babasaheb Ambedkar Marathwada University, Aurangabad (MS), India
[2] Department of Chemical and Environmental Engineering, University of California, Riverside, CA, USA
[3] Department of Chemistry, Hanyang University, Seoul, South Korea
[4] The Center for International Cooperation Engineering Education (CICEE), The University of Tokushima, Tokushima, Japan

E-mail: mds_bamu@yahoo.co.in and mdshirsat@gmail.com

Received 16 August 2013, in final form 29 September 2013
Published 19 November 2013
Online at stacks.iop.org/JPhysD/46/495110

Abstract
We report the fabrication and characterization of poly(*N*-methylpyrrole) nanowires electrode junction based back-gated field-effect transistors under varying dopant atmosphere. Influences of the anionic radius of dopants on electrochemical, morphological, spectroscopic and electrical characteristics of synthesized nanowires have been investigated. The FET measurements have revealed highly efficient gate induced modulation of the channel conduction behaviour for all dopant cases and characteristic FET parameters have been estimated. The best observed device in terms of charge carrier mobility $(\mu) = 4.54 \times 10^{-4}\,\mathrm{cm^2\,V^{-1}\,s^{-1}}$ and on-off ratio $(I_{on}/I_{off}) = 8.5 \times 10^3$ could be characterized with NaOH as dopant. Observed behaviour of the FET devices has been rationally related to the anionic radius of dopants. Plausible interpretation reflects that dopant dimension can be a significant and facile tool for optimized designing of polymeric FETs.

(Some figures may appear in colour only in the online journal)

1. Introduction

Since the first ever demonstration by Koezuka and co-workers in 1987 [1, 2], organic field-effect transistors (OFETs) have come a long way to emerge as a potential solution for the highest demanding sectors, ranging from cost effective organic electronics [3, 4] to miniaturized sensing platforms [5, 6]. Such drastic developments have been made possible due to several fundamental issues that include low cost, ease of processabilty, and suitability of this class for large-area electronics [7, 8]. To attain the present stature of FETs based on polycrystalline silicon, there is a continuous drive for improvement especially of charge mobility, on/off ratio and threshold voltage in OFETs [9–12]. A large spectrum of efforts towards this aim includes pursuit of chemically engineered novel active materials [10, 13], physical modifications of channel [14] and strategically manoeuvered dielectric materials [15, 16]. From a widespread choice of active materials for OFETs, conducting polymers (CPs) have gained substantial attention due to: (i) tunable charge transport property of CPs that enables efficient control over the key performance parameters of OFETs, and (ii) flexibility in techniques available to synthesize polymeric materials with excellent spatial control. Several technologically important polymers, e.g. poly(aniline) [17], poly(pyrrole) [18, 19], derivatives of poly(thiophene) [20, 21] etc, have been employed as active materials in OFETs. 1D formations of CPs or CP nanowires are technically more appealing than thin-film structures as active materials since in the latter, fast charge kinetics is impeded by misalignment of polymers leading to less than ideal efficiency [22]. Employing CPs as active materials in OFETs has an exclusive advantage since, during synthesis, a wide range of dopants can be employed for obtaining, especially, requisite electronic and electrical properties [23–26]. Mobility in polymeric FETs has been reported to be increased by several orders by varying

[5] These authors contributed equally.
[6] Author to whom any correspondence should be addressed.

the dopant concentration [27]. Not much effort, however, has been directed to explore this facile route towards tunable FET devices.

Fabrication of a polymeric nanowire based FET device is generally constituted of two steps, i.e. synthesis of the nanowires followed by their introduction onto lithographically patterned electrodes on suitable substrates (most generally, Si/SiO_2). The pursuit for a direct fabrication modality leads to a template free, site-specific electrochemical route for deposition of dendritic polymeric nanowires matrix between pre-patterned electrodes (2 μm separation) demonstrated by Wang *et al* [28]. This method is appealing due to the inherent simplicity, and was further extended by Alam and co-workers [29] towards fabrication of electrolyte gated transistors based on individually addressable conducting polymer nanowires on electrode junctions (CPNEJs; as the name coined by authors) in an array of microfabricated electrodes on a single platform. Although charge kinetics in such platforms is a debatable issue due to numerous crossing or intertwine of the nanowires, factors such as robustness of polymer-electrode contacts, ease of synthesis and substantial control over the diametric distribution of nanowires have attracted researchers to explore such backbones for practical applications [30]. However, CPNEJs based back-gated FET structure, particularly from a device perspective, is less reported, and the present work embodies our initial observations on this line of investigation being carried out by our group. The present investigation is not framed with sheer intention towards development of OFETs with exclusive properties, rather applicability of CPNEJs as back-gated FET devices was examined and particularly, some control modality over synthesized FETs performance was sought. The most fascinating outcome of the study lies in the achievement of a significant manoeuverability on overall performance of the synthesized devices by employing dopants of different anionic radii for synthesis of the polymeric nanowires platforms.

In the present investigation, the authors have synthesized CPNEJs based FETs of poly(N-methyl pyrrole) [P(NMP)] bridging a 3 μm gap between two micropatterned Au electrodes on a Si/SiO_2 substrate where the heavily doped $Si(P^+)$ acts as the back gate. P(NMP) was a choice as active material due to its low susceptibility towards oxygen and humidity [31] that is expected to render less drift in FET performance with time. During templateless onsite electrochemical synthesis of the nanowires, dopants with various anionic radii have been employed. In ascending order of anionic radii, the dopants used for the present study can be enlisted as: sodium hydroxide (OH^- ~133 pm) < hydrochloric acid (Cl^- ~164 pm) < sodium nitrate (NO_3^- ~179 pm) [32] (all small sized anions)≪para toluene sulphonic acid (TsO^-; medium sized anion) [33, 34]. Apart from FET studies, comparative electrical and spectroscopic studies have been carried out. Our observations show that dopant dimension has an important role in shaping these properties.

2. Experimental details

2.1. Materials

N-methyl pyrrole (NMP; >99%) was obtained from ACROS-ORGANICS (Geel, Belgium). Dopants sodium hydroxide (NaOH), hydrochloric acid (HCl), sodium nitrate ($NaNO_3$) and para toluene sulphonic acid (PTSA) were procured from RANKEM, India. The monomer was vacuum distilled prior to use and the rest of the chemicals were used as-received.

2.2. CPNEJ OFET synthesis and characterizations

For site-specific synthesis of the P(NMP) nanowires between pre-defined Au microelectrode patterns (acting as source and drain) on Si/SiO_2 substrate, two-step galvanostatic deposition route [30] was adapted. Au microelectrode patterns were photolithographically transferred on heavily doped (P^+) substrate with a thermally grown oxide layer (300 nm). A 20 nm Cr adhesive layer and 180 nm Au layer were finally deposited by successive e-beam and thermal evaporation. A generic three-electrode set-up was framed by externally shorting two consecutive Au microelectrodes while a Pt wire [CH Instruments; CHI115] and a chlorinated Ag wire acted as counter and pseudo reference electrode, respectively [35]. The Au microelectrodes were wire bonded [West Bond; 7476D] allowing connection to galvanostat (CH Instruments; CHI660C) and further electrical measurements. Epoxy glue was stamped onto the bonded regions and part of microelectrodes to reduce the effective working area of the electrode [36] to about 39,154 μm^2. The electrolyte solutions contained monomer and respective dopant at a concentration ratio of 0.25mM : 0.1mM in HPLC grade water (Rankem, India). A 0.2 μl de-aerated electrolytic solution was dispensed onto the Au 'fingertips' region. The counter and reference electrodes were precisely poised in contact to the electrolyte via probe-station (Ecopia; EPS1000). Schematics of the nanowires synthesis platform and three-electrode set-up is shown in figures 1(*a*) and (*b*), respectively. The typical two-step deposition process consisted of 0.05 mA cm^{-2} anodic current density for 20 min followed by 0.02 mA cm^{-2} for 90 min applied to the working electrodes at room temperature.

Surface morphology of the CPNEJs was examined by field-emission scanning electron microscopy (FESEM; Hitachi S4800). I–V characteristics were studied by linearly sweeping potential from −1 to +1 V (CHI660C). Spectroscopic data were recorded by UV–VIS spectrophotometer (Shimadzu; UV 2450). FET characteristics (output and transfer) in back-gated modality were recorded with a Keithley 2636A dual channel source measure unit. For studying the output characteristics, drain-to-source voltage (V_{DS}) was swept from 0 to −25 V at various gate to source voltages (V_{GS}). Transfer characteristics were obtained by sweeping the V_{GS} from −20 V to +20 V while keeping the V_{DS} fixed at −10 V. The I–V and FET measurements were carried out under general laboratory conditions.

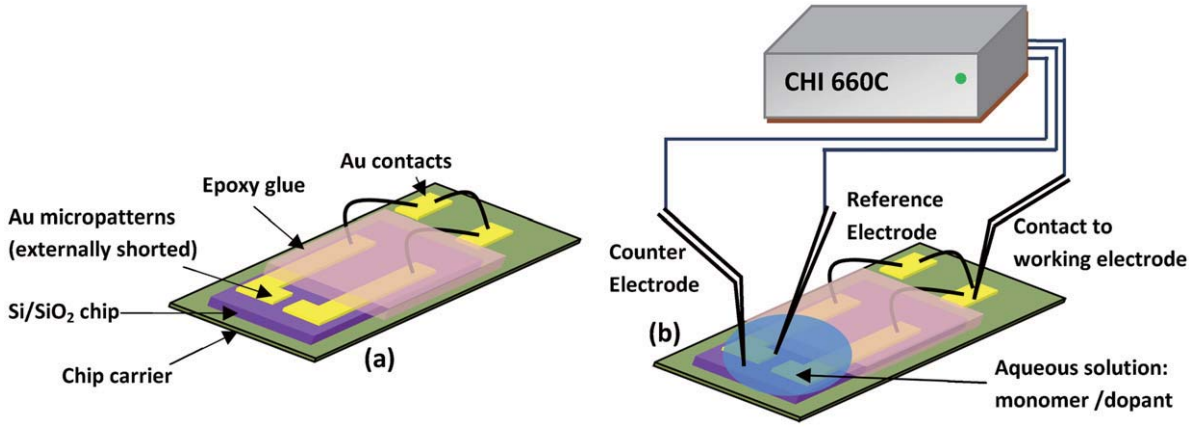

Figure 1. Schematics of the nanowires synthesis platform; (*a*) epoxy coated Si/SiO_2 chip, wire bonded to external contacts; and (*b*) three-electrode set-up, in contact with electrolyte solution.

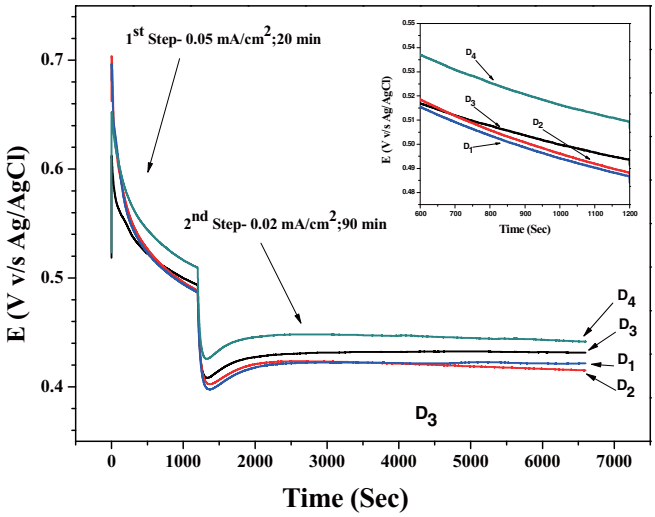

Figure 2. Chronopotentiograms for two-step galvanostatic synthesis of P(NMP) nanowires with various dopants; (inset) magnified view of plateau regions in first step of polymerization.

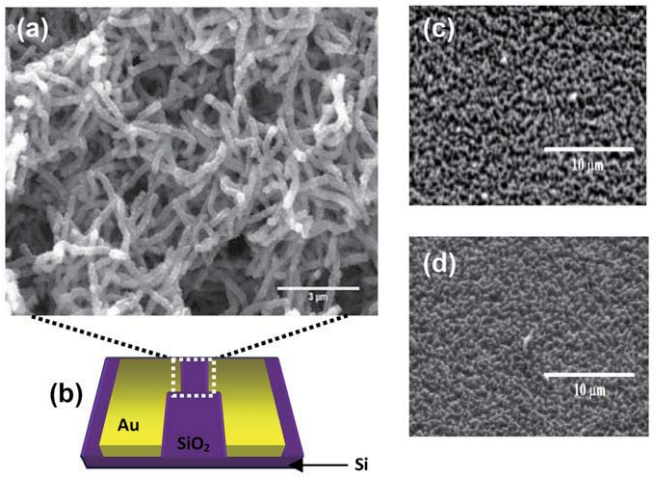

Figure 3. (*a*) Typical FESEM image of P(NMP) nanowires synthesized with NaOH as dopant and electrochemical parameters as stated in section 2.2; (*b*) graphical representation of the Au microelectrodes (3 μm apart) pattern on Si/SiO_2 substrate; (*c*) and (*d*) show FESEM images of P(NMP) nuclei after the completion of first step of deposition at current densities 0.05 mA cm^{-2} and 0.02 mA cm^{-2}, respectively

3. Results and discussion

3.1. Electrochemical synthesis and morphological study

Chronopotentiograms for the onsite synthesis of P(NMP) nanowires devices with different dopants are shown in figure 2. During the first step of the two-step polymerization, effective potential at the working electrode were found to be lying in the range 0.5–0.47 V for different dopants. Customarily, the first step of a two-step polymerization process comprises a comparatively higher current density and is responsible for the formation of polymer nuclei that acts as seeds for further growth. On lowering the current density in the second step, the potential of the working electrode decreased and finally stabilized at about 0.44 V to 0.40 V, indicating the formation of nanowires [22]. The polymerization potential (measured at the plateau region of the first step) of different doped devices followed the order-P(NMP)/NaOH< P(NMP)/HCl< P(NMP)/$NaNO_3$ < P(NMP)/PTSA (to be denoted by D_1, D_2, D_3, D_4, respectively, hereafter).

This observation is suggestive of a reverse trend in conductivity levels of the synthesized devices since a higher polymerization potential is reported to result in lower conductivity [37].

Figure 3(*a*) illustrates FESEM image of the P(NMP) nanowires synthesized with NaOH as dopant that shows formation of dendritic nanowires with abundant intertwines. A typical 3-D representation of the Au fingertips on Si/SiO_2 substrate that served as the platform for formation of CPNEJs is shown in figure 3(*b*). The average diametric distribution of the nanowires was found to lie in the range of 250–300 nm. The surface of the synthesized nanowires is found to be smooth and uniform by and large. Similar morphology of electrochemically synthesized P(NMP) nanowires has been reported earlier by the authors [35]. Usually, in polymeric thin films, dopants are reported to have substantial effects on morphology of the film [25]. However, in the present case, more or less similar characteristic morphology could be

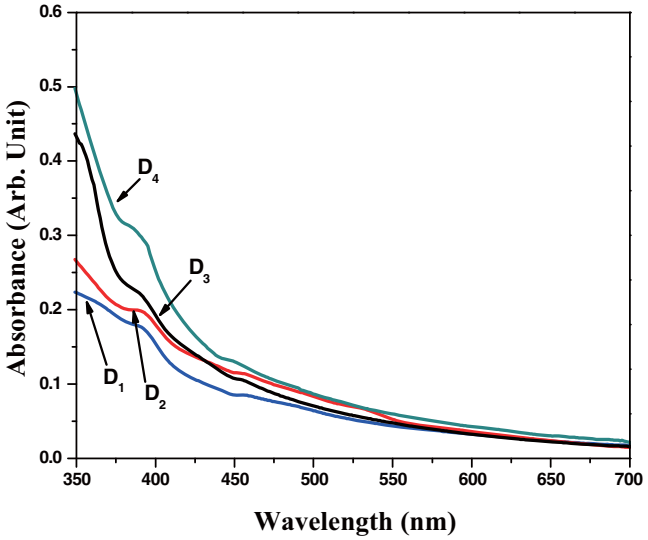

Figure 4. UV–visible spectra of P(NMP) nanowires with various devices.

observed with other devices (i.e. D_2, D_3 and D_4; data not shown). Figures 3(*c*) and (*d*) show formation of P(NMP) nuclei after first step of polymerization. The dopant used was NaOH and the current densities applied were 0.05 mA cm^{-2} and 0.02 mA cm^{-2} (20 min duration in each case), respectively. It is clearly visible from the figures that changing the current density results in different diameters of the nuclei (average diameter about 200 nm in first case and about 115 nm in the second case). Such observations indicate that the applied current density in the first step of a two-step galvanostatic synthesis of nanowires may play a key role in deciding diameter of the yield. Further investigation in this direction is warranted.

3.2. Electronic spectroscopy studies

Figure 4 shows the UV–Vis spectra of doped P(NMP) nanowires. The spectra are dominated by two absorption peaks around 390 nm and 455 nm, respectively. The 390 nm absorption band is assigned to π–π^* electronic transition of the conjugated C=C chain [38, 39]. The position of this peak is related to degree of conjugation between adjacent rings in the polymer chain [40]. Although, PTSA renders efficient wavefunction overlap by dint of their structural feature, our observations reveal that the rest of the dopants achieve better conjugation than PTSA. The hump around 455 nm band is attributed to high energy polaron transition [41, 42] which is indicative to the protonation of polymeric backbone [43]. The band gap values for π–π^* transitions corresponding to the first absorption band were calculated by formula $\Delta E = hc/\lambda_{\pi-\pi^*}$ ($h = 6.625 \times 10^{-34}$ J s and $c = 3 \times 10^8$ ms^{-1}) [25] and are furnished in table 1. A steady blue shift could be observed in the π–π^* transition wavelength in accord with the increase in ionic radii of the dopants and accordingly the band gap values were found to be ordered.

3.3. Electrical and FET measurements

I–*V* characteristics of the P(NMP) nanowire based devices are shown in figure 5. For all dopant cases, the current and

Table 1. $\lambda_{\pi-\pi^*}$, band gap values of synthesized P(NMP) nanowires with various dopants and resistance of corresponding devices.

Device	$\lambda_{\pi-\pi^*}$ (nm)	Band gap (eV)	Resistance (MΩ)
D_1	394.21	3.15	12.72
D_2	391.91	3.17	16.58
D_3	390.68	3.18	17.54
D_4	384.63	3.23	19.26

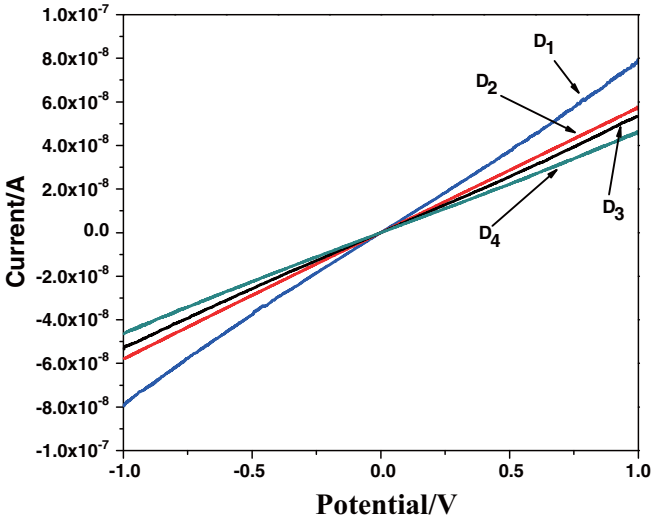

Figure 5. Room temperature *I*–*V* characteristics of P(NMP) nanowires devices.

voltage displayed a linear and symmetric relation confirming formation of ohmic contacts. Thus, it is established that the work function of the synthesized polymeric nanowires matrix lies below that of the contact metal i.e. Au ($\phi_{Au} = 5.1$ eV) [43]. Resistance of the devices was determined by taking the inverse of the slope of *I*–*V* curve and is presented in table 1. Resistance of different doped devices followed the order $D_1 < D_2 < D_3 < D_4$ that is in agreement to the band gap values and electrochemical data obtained. Such observations are clearly indicative of the fact that the ionic size of the anions used for the present investigation (as dopants) plays an instrumental role in deciding the electrical behaviour of the polymeric devices.

The typical output characteristics are shown in figures 6(*a*)–(*d*) of the P(NMP) nanowires FET devices under various dopant conditions. In all cases, p-type nature is evident with clear linear and saturation regime of operation. Thus, changing the anionic radius did not affect the basic FET characteristics. Highest saturation current could be observed with NaOH as dopant. Also, the peak saturation current (I_P) level followed the order $D_1 > D_2 > D_3 > D_4$ that is well in agreement with the electrochemical, spectral and *I*–*V* studies in the present investigation. The pinch off voltage (V_P) is found to decrease with increase of anionic radii of employed dopants and the lowest pinch off voltage could be recorded for PTSA as dopant.

The observations suggest that optimization of the anionic radius can be an effective route for acute control of I_P and V_P of such devices.

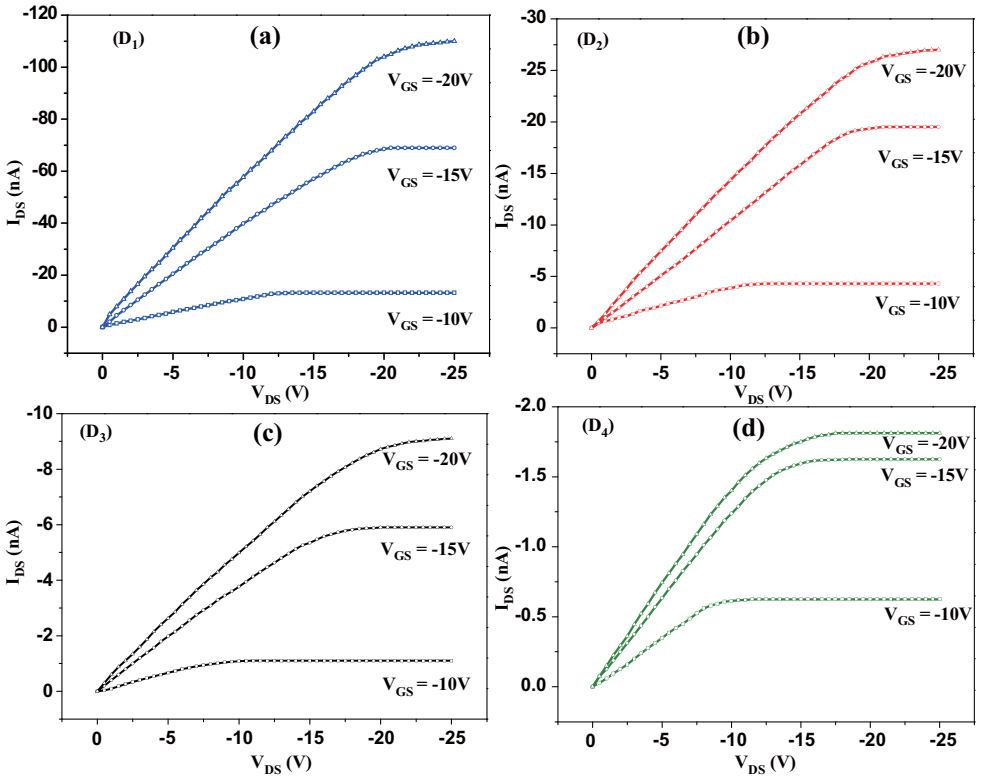

Figure 6. Output characteristics of (*a*) D_1, (*b*) D_2, (*c*) D_3, (*d*) D_4 for different V_{GS} values.

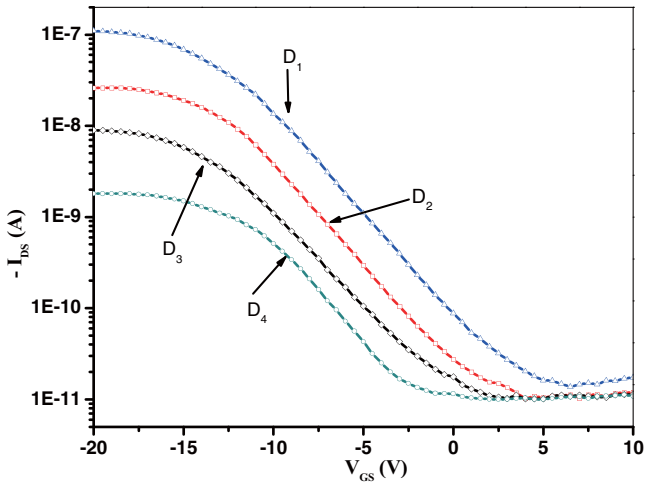

Figure 7. Transfer characteristics of the fabricated devices.

The transfer characteristics of the devices recorded at constant $V_{DS}(-10\,V)$ are given in figure 7. In comparison to earlier reported electrolyte gated CPNEJs based FETs [29] and polymeric single nanowire based FET devices [44], substantially lower off-state current (about two orders of magnitude) and better switching behaviour have been exhibited by the present devices. A regular shift in threshold voltage (V_{TH}) towards more positive values could be observed with decrease in anionic radius of the dopant.

The device carrier mobility values (μ) were calculated by using the formula $\mu = L_{SD}^2\,gm/C_G V_{DS}$ [45]. For the estimation of mobility, full parallel plate gate capacitance was used i.e. $C_G = \varepsilon W L_{SD}/L_{OX}$ ($W = 200\,\mu m$, $L_{SD} = 3\,\mu m$, $L_{OX} = 300\,nm$) and transconductance ($gm = dI/dV_g$) of the respective devices were estimated in the linear regime of device operation. In line with our earlier observations, the P(NMP)-NaOH device exhibited the highest carrier mobility that has resulted in higher magnitude of on current and subsequently, highest on-off ratio (I_{on}/I_{off}) [46].

The maximum and average values (for at least seven devices in each case) of mobility and on-off ratio of all devices measured are summarized in figure 8. A significantly low device-to-device variation could be observed for all dopant cases.

The evident regularity in our experimental observations was highly supportive towards correlation of the same with the anionic radius of the dopants. For elucidation of the conduction behaviour of the synthesized devices in different dopant condition, typical conduction phenomenon in polymeric material was considered. The conduction mechanism in a polymer is dependent on both intrachain and interchain hopping of charge carriers. However, only a small amount of charge carriers are mobile since most of them are self-trapped by dint of coulombic attraction to their counterions (i.e. dopant anions) [27]. Such electrostatic force of attraction is certain to be higher for anions with smaller radius, resulting in higher trapping of charge carriers in comparison to larger sized anions. Probably, this anionic radius dependent variation in trapping mechanism has defined the intermediate localized states [46] in the gap between valence and conduction bands and shaped the band gap structure of the synthesized nanowires. The band gap values also suggest higher order conjugation between adjacent

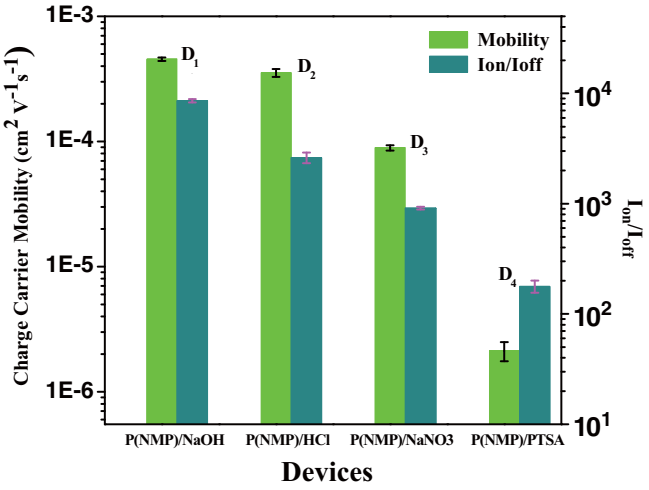

Figure 8. Mobility and on/off ratio of the fabricated devices (at least seven devices have been tested in each case).

polymeric rings with decreasing anionic radius that indicates concurrent decrease in hopping length.

In polymeric FET structures, accumulated charges are supposed to experience less electrostatic attraction since Coulombic traps are already filled by self-trapped charges induced by dopants [27]. As already discussed, such an effect is profuse for smaller anions that may result in higher density of free charged carriers and at the same time, facilitate intra and interchain hopping phenomenon. Smaller conjugation length suggested by spectroscopic data, in the case of small anionic dopants, also accounts for the observed conduction behaviour. However, from the above perspective, dopants with higher anionic radii are supposed to render less electrostatic attraction which contradicts the above possible explanation, and also the experimental observations. Therefore, the poor conduction/FET characteristics for higher sized dopants may be attributed to: (i) higher trapping probability for accumulated charge carriers since Coulombic traps are less filled, and (ii) the deterioration of ordering in polymers chains leading to lower crystallinity and enhanced interchain separation [25] making the interchain hopping increasingly difficult. Finally, the changes observed in the values of V_{TH} with various dopants, could be well rationalized by considering the channel and the back gate as two plates of a parallel plate capacitor separated by dielectric layer [47]. This model suggests that for a p-type material, applied gate potential needs to be shifted to increasing positive values to deplete the channel if charge carrier density increases and such occurrence are well in line with our observations, as discussed earlier.

4. Conclusions

To conclude, electrochemistry provides a simple route towards fabrication of back-gated FET structures based on CPNEJs. P(NMP) nanowires based organic FETs, under all dopant conditions, were characterized with efficient modulation in channel conduction behaviour upon changing of gate potential. By employing dopants with various anionic radii, the characteristic parameters of the fabricated devices (viz carrier mobility, on-off ratio, threshold voltage, forward current and pinch-off voltage) could be altered, and most encouragingly, such changes exhibited a regular trend as a function of dopant anionic radius. The observations could be rationalized in terms of hopping phenomenon under the field of Coulombic attraction rendered by respective counterions. The spectral and I–V data were highly supportive in figuring a possible explanation for the observed device characteristics. The fabricated devices exhibited p-type nature with significant levels of charge carrier mobility and on-off ratio factors. Changing anionic radius, therefore, may be treated as an efficient route to manoeuver operational efficiency of polymeric FETs. Although, the term 'predictive' seems to be optimistic at this moment, yet, a database on similar materials will definitely come in handy for long-term applications.

Acknowledgments

Authors (KD, PG, MDS) are thankful to Department Of Science and Technology (DST)—Nanomission, New Delhi, India (Grant No SR/NM/NS-94/2009), Department Of Science and Technology (DST)—TSD, New Delhi, India (Grant No DST/TSG/PT/2010/11-C & G) and Inter University Accelerator Centre (IUAC), New Delhi, India (Grant No IUAC/XIII.7/UFR-48309/984) for financial assistance.

References

[1] Koezuka H, Tsumura A and Ando T 1987 *Synth. Met.* **18** 699–704
[2] Tsumura A, Koezuka H and Ando T 1988 *Synth. Met.* **25** 11–23
[3] Forrest S R 2004 *Nature* **428** 911–8
[4] Kim S H, Hong K, Xie W, Lee K H, Zhang S, Lodge T P and Frisbie C D 2013 *Adv. Mater.* **25** 1822–46
[5] Diallo K, Lemiti M, Tardy J, Bessueille F and Renault N J 2008 *Appl. Phys. Lett.* **93** 183305
[6] Shirale D J, Bangar M A, Chen W, Myung N V and Mulchandani A 2010 *J. Phys. Chem.* C **114** 13375–80
[7] Dimitrakopoulos C D and Malenfant P R L 2002 *Adv. Mater.* **14** 99–117
[8] Arias A C, MacKenzie J D, McCulloch I, Rivnay J and Salleo A 2010 *Chem. Rev.* **110** 3–24
[9] Kraus M, Richler S, Opitz A, Brutting W, Haas S, Hasegawa T, Hinderhofer A and Schreiber F 2010 *J. Appl. Phys.* **107** 094503
[10] Liu S, Mannsfeld S C B, LeMieux M C, Lee H W and Bao Z 2008 *Appl. Phys. Lett.* **92** 053306
[11] Wang Y, Liu Y, Song Y, Ye S, Wu W, Guo Y, Di C, Sun Y, Yu G and Hu W 2008 *Adv. Mater.* **20** 611–5
[12] Bo X Z, Lee C Y, Strano M S, Goldfinger M, Nuckolls C and Blanchet G B 2005 *Appl. Phys. Lett.* **86** 182102
[13] Huang J, Hines D R, Jung B J, Bronsgeest M S, Tunnell A, Ballarotto V, Katz H E, Fuhrer M S, Williams E D and Cumings J 2011 *Org. Electron.* **12** 1471–6
[14] Uno M, Hirose Y, Uemura T, Takimiya K, Nakazawa Y and Takeya J 2010 *Appl. Phys. Lett.* **97** 013301
[15] Wang A, Kymissis I, Bulovic V and Akinwande A I 2006 *Appl. Phys. Lett.* **89** 112109
[16] Klauk H, Halik M, Zschieschang U, Schmid G, Radlik W and Weber W 2002 *J. Appl. Phys.* **92** 5259–63
[17] Kuo C T and Chiou W H 1997 *Synth. Met.* **88** 23–30

[18] Bof Bufon C C and Heinzel T 2006 *Appl. Phys. Lett.* **89** 012104
[19] Xue F, Su Y and Varahramyan K 2004 *MRS Proc.* 814 I10.20 DOI:10.1557/PROC-814-I10.20
[20] Hines D R, Southard A and Fuhrer M S 2008 *J. Appl. Phys.* **104** 024510
[21] Fu Y, Lin C and Tsai F Y 2009 *Org. Electron.* **10** 883–8
[22] Liang L, Liu J, Windisch C F Jr, Exarhos G J and Lin Y 2002 *Angew. Chem. Int. Edn Engl.* **41** 3665–8
[23] MacDiarmid A G 2001 *Angw. Chem. Int. Edn Engl* **40** 2581–90
[24] Heeger A J 2001 *Angw. Chem. Int. Edn Engl* **40** 2591–611
[25] Sinha S, Bhadra S and Khastgir D 2009 *J. Appl. Polym. Sci.* **112** 3135–40
[26] Lippe J and Holze R 1992 *J. Electroanal. Chem.* **339** 411–22
[27] Brown A R, Leeuw D M, Havinga E E and Pomp A 1994 *Synth. Met.* **68** 65–70
[28] Wang J, Chan S, Carlson R R, Luo Y, Ge G, Ries R S, Heath J R and Tseng H R 2004 *Nano Lett.* **4** 1693–7
[29] Alam M M, Wang J, Guo Y, Lee S P and Tseng H R 2005 *J. Phys. Chem.* B **109** 12777–84
[30] Shirsat M D, Bangar M A, Desshusses M A, Myung N V and Mulchandani A 2009 *Appl. Phys. Lett.* **94** 083502
[31] Kanazawa K K, Diaz A F, Korunbi M T and Street G B 1981 *Synth. Met.* **4** 119–30
[32] Volkov A G, Paula S and Deamer D W 1997 *Bioelectroch. Bioener.* **42** 153–60
[33] Qi K, Chen Z, Zhang G and Guo X 2011 *Open Corros. J.* **4** 18–26
[34] Johanson U, Marandi M, Tamm T and Tamm J 2005 *Electrochim. Acta* **50** 1523–8
[35] Datta K, Ghosh P, More M A, Shirsat M D and Mulchandani A 2012 *J. Phys. D: Appl. Phys.* **45** 355305
[36] Wang Y, Coti K K, Wang J, Alam M M, Shyue J J, Lu W, Padture N P and Tseng H R 2007 *Nanotechnology* **18** 424021
[37] Shirale D J, Gade V K, Gaikwad P D, Kharat H J, Kakde K P, Savale P A, Hussaini S S, Dhumane N R and Shirsat M D 2006 *Mater. Lett.* **60** 1407–11
[38] Inoue T and Yamase T 1983 *Bull. Chem. Soc. Japan.* **56** 985–90
[39] Kim D Y, Lee J Y, Moon D K and Kim C Y 1995 *Synth. Met.* **69** 471–4
[40] Pron A and Rannou P 2002 *Prog. Polym. Sci.* **27** 135–90
[41] Bredas J L, Scott J C, Yakushi K and Street G B 1984 *Phys. Rev.* B **30** 1023–5
[42] Zotti G and Schiavon G 1989 *Synth. Met.* **30** 151
[43] Elmansouri A, Outzourhit A, Lachkar A, Hadik N, Abouelaoualim A, Achour M E, Oueriagli A and Ameziane E L 2009 *Synth. Met.* **159** 292–7
[44] Wanekaya A K, Bangar M A, Yun M, Chen W, Myung N V and Mulchandani A 2007 *J. Phys. Chem.* C **111** 5218–21
[45] Rushi A, Datta K, Ghosh P and Shirsat M D 2013 *Mater. Lett.* **96** 38–41
[46] Horowitz G 1998 *Adv. Mater.* **10** 365–77
[47] Braga D and Horowitz G 2009 *Adv. Mater.* **21** 1473–86